Optomechanical Sensing of Spontaneous Wave-Function Collapse

Stefan Nimmrichter,[1] Klaus Hornberger,[1] and Klemens Hammerer[2]

[1]*Faculty of Physics, University of Duisburg-Essen, Lotharstraße 1, 47048 Duisburg, Germany*
[2]*Institute for Theoretical Physics and Institute for Gravitational Physics (Albert Einstein Institute),*
Leibniz University Hannover, Callinstraße 38, 30167 Hannover, Germany

Quantum experiments with nanomechanical oscillators are regarded as a test bed for hypothetical modifications of the Schrödinger equation, which predict a breakdown of the superposition principle and induce classical behavior at the macroscale. It is generally believed that the sensitivity to these unconventional effects grows with the mass of the mechanical quantum system. Here we show that the opposite is the case for optomechanical systems in the presence of generic noise sources, such as thermal and measurement noise. We determine conditions for distinguishing these decoherence processes from possible collapse-induced decoherence in continuous optomechanical force measurements.

Introduction.—The observation of quantum behavior in a growing number of macroscopic systems of light or matter has demonstrated the validity of the superposition principle at impressively large scales [1–4]. Within the framework of quantum mechanics the disappearance of coherent superposition states at macroscopic scales is attributed entirely to the interaction with uncontrolled and unobserved degrees of freedom. This is the paradigm of decoherence theory [5–7]. According to alternative approaches, quantum theory must be modified at a fundamental level to explain the emergence of macroscopic realism [8] and to solve the measurement problem [9]. Such modifications are designed to induce an objective collapse of the wave function above a critical mass scale of a given quantum system, thereby restoring classicality.

The most widely studied modification is the model of continuous spontaneous localization (CSL) [9–11], which introduces a nonlinear stochastic addition to the Schrödinger equation. The delocalized wave function of a massive particle gets gradually and randomly localized down to a microscopic length scale of about 100 nm, at a rate that amplifies with the particle's mass. In many respects, the CSL model can be regarded as the prime example of a broad generic class of macrorealist modifications; it is compatible with all experimental observations to date and with most of the symmetry principles underlying both quantum and classical mechanics [9,12,13]. Another important macrorealist model is the Diósi-Penrose (DP) collapse mechanism [11,14–16], which explains the effect by gravitational self-interaction.

The main prediction of these models is the objective breakdown of the quantum superposition principle with growing mass. This would be directly observable by a specific mass-dependent loss of visibility in interference experiments with nanoparticles [17–21]. However, the mass range where macrorealistic collapse should become effective has yet to be reached in experiments.

At the same time, the random localization process predicted by the CSL (and the DP) model inherently implies momentum diffusion, i.e., a Brownian-like background noise, which also affects the classical motion of macroscopic matter. No quantum coherence is required to detect these hypothetical sources of noise [22]. In fact, the necessary tools are being used in optomechanics labs worldwide: nano- and micromechanical oscillators manipulated and readout by optical fields are the most sensitive measurement devices for forces [23–26]. Recent experiments have demonstrated measurement sensitivities limited by radiation-pressure backaction noise [27–30], a necessary condition for reaching the standard quantum limit of continuous force measurements [31,32]. Such measurements can give rise to Gaussian entangled states of macroscopic masses [33], which can be used to test DP models [34].

In this Letter, we assess the requirements for detecting the force noise postulated by macrorealistic models in optomechanical devices. We show that ultrasensitive force measurements at cryogenic temperatures using oscillators with low (sub-Hz) resonance frequencies, subgram masses, and high mechanical quality factors can test significant and unexplored parameter regimes of those models. Surprisingly, we find that *higher* masses will in general imply *lower* sensitivities.

Our results serve also as a benchmark for optomechanical superposition experiments [17–19,21]. The tiny oscillation amplitudes of such oscillators (on the scale of femto- to picometers) allow the collapse modification to be approximated by a linear diffusion term. The coherence loss rate for all superposition states is therefore determined by the same momentum diffusion rate that governs motional noise [35]. In the following, we focus on the CSL model, and state the analogous DP results only in the end.

Noise induced by localization.—The CSL model is characterized by two parameters, the localization length

r_{CSL} and the localization rate λ_{CSL}. The former, convention-ally set to the value $r_{CSL} = 100$ nm, determines the size down to which delocalized quantum states get localized. The latter gives the average localization rate at one proton mass; it is currently believed not to exceed $10^{-8\pm2}$ Hz [11,36,37]. The challenge is to identify experimental test beds where the localization rate λ_{CSL} can be sensed at this level [38].

The effective localization and diffusion rates of many-body systems amplify with mass, and they depend on the spatial extension of both the quantum state of motion and the mass distribution. Two regimes can be considered: For nanoparticles smaller than r_{CSL} prepared in super-position states with separations larger than r_{CSL}, as relevant to matter-wave interferometry, the effective coherence loss rate grows in proportion to the squared mass [9,19,39]. On the other hand, for micrometer-sized mechanical resonators delocalized over amplitudes much smaller than r_{CSL}, as relevant in optomechanics, we find a *sublinear* mass scaling of the effective localization and diffusion rate. To be specific, let us focus on cantilever configurations, where the center of mass of a rigid body of mass m oscillates linearly, say, along the x axis with an amplitude $x_0 \ll r_{CSL}$. This could be a cubic mirror [17], an optically trapped nanosphere [40,41], or a micromembrane [42,43]. In this limit, the observable consequences of the CSL model are approximated by a quantum master equation $\dot{\rho} = (\mathcal{L} + \mathcal{L}_{CSL})\rho$, where $\mathcal{L}$ is a Liouvillian associated to standard quantum mechanics. The Lindblad term $\mathcal{L}_{CSL}\rho = -D_{CSL}[x,[x,\rho]]/\hbar^2$, with x the center-of-mass position operator, describes the momentum diffusion implied by the CSL modification. It can be viewed as arising from a stochastic force $f_{CSL}(t)$ characterized by the two-time correlation function $\langle f_{CSL}(t)f_{CSL}(t')\rangle = D_{CSL}\delta(t-t')$. The associated diffusion rate $D_{CSL} = \lambda_{CSL}(\hbar/r_{CSL})^2\alpha$ involves a mass-dependent geometry factor [44],

$$\alpha = \frac{r_{CSL}^5}{\pi^{3/2}\,\text{amu}^2}\int d^3k\, k_x^2 e^{-r_{CSL}^2 k^2}|\tilde{\varrho}(\mathbf{k})|^2. \quad (1)$$

Here, $\tilde{\varrho}(\mathbf{k}) = \int d^3r\varrho(\mathbf{r})e^{-i\mathbf{k}\cdot\mathbf{r}}$ denotes the Fourier transform of the mass density, normalized to the total mass, $\tilde{\varrho}(0) = m$. The cantilever can safely be described as a homogeneous rigid body since the dynamics and structure of the underlying crystal lattice vary well below the scale of $r_{CSL} = 100$ nm. Simple expressions for the geometry factor (1) are then obtained for materials with a constant mass density ϱ and dimensions greater than r_{CSL} [44]. In the case of spheres and cubes with radii $R \gg r_{CSL}$ and side lengths $b \gg r_{CSL}$, we find

$$\alpha_{\text{sph}}(R) \approx \frac{16\pi^2\varrho^2 r_{CSL}^4}{3\,\text{amu}^2}R^2, \quad \alpha_{\text{cube}}(b) \approx \frac{8\pi\varrho^2 r_{CSL}^4}{\text{amu}^2}b^2, \quad (2)$$

both proportional to $m^{2/3}$ at fixed ϱ. For the motion of a thin membrane (thickness $d \ll r_{CSL}$, radius $R \gg r_{CSL}$) along its symmetry axis, we obtain

$$\alpha_{\text{disk}}(R) \approx \frac{2\pi^2\varrho^2 r_{CSL}^2}{\text{amu}^2}d^2R^2. \quad (3)$$

Keeping the density and thickness fixed, the radius scales like $R = \sqrt{m/\pi\varrho d}$, and the geometry factor is at best proportional to mass. Exact geometry factors are derived in the Supplemental Material [44,45].

CSL in the presence of thermal diffusion.—The overall sublinear increase of the geometry factors with mass must be put into perspective by comparing CSL diffusion to standard sources of noise, most prominently, thermal noise. The mechanical motion in a thermal environment, and including the CSL effect, is sketched in Fig. 1. It is described by the Langevin equations of motion

$$\dot{x} = p/m, \qquad \dot{p} = -m\Omega^2 x - \gamma p + f_T(t) + f_{CSL}(t), \quad (4)$$

where Ω and γ are the mechanical resonance frequency and line width, respectively. The thermal noise force $f_T(t)$ is characterized by $\langle f_T(t)f_T(t')\rangle = D_T\delta(t-t')$ and $D_T = 2\gamma m k_B T$, valid in the relevant high-temperature limit $k_B T \gg \hbar\Omega$ of the environmental bath.

The CSL momentum diffusion would dominate over thermal diffusion, and would thus be detectable in the noise spectrum, if $D_{CSL} > D_T$, i.e.,

$$\Lambda_T \equiv \frac{2r_{CSL}^2\gamma k_B T}{\hbar^2}\frac{m}{\alpha} < \lambda_{CSL}. \quad (5)$$

This condition gives a lower bound Λ_T of CSL rate parameters for which the localization effect would be observable on top of the thermal noise spectrum; a significant test should aim for values between 0.1 nHz and 1 μHz.

Quite remarkably, the generally sublinear mass scaling of the geometry factors implies that more sensitive tests of the rate parameter require *smaller* test masses (as long as the object stays larger than $r_{CSL} = 100$ nm). This is in strong contrast to the quadratic enhancement of CSL
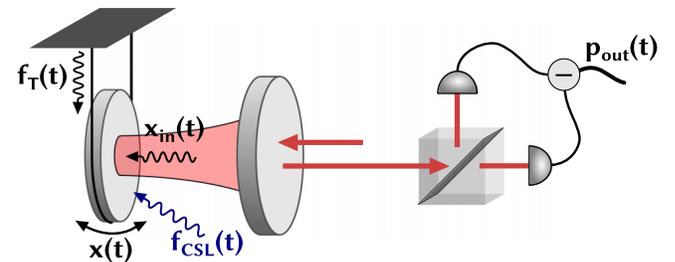

FIG. 1 (color online). Sketch of an optomechanical setup for measuring macrorealistic noise forces. The harmonic motion $x(t)$ of a cantilever, monitored by means of an optical cavity field, is subject to thermal noise $f_T(t)$, optical amplitude noise $x_{in}(t)$, and a hypothetical collapse-induced noise force $f_{CSL}(t)$. All three contributions are reflected in the noise spectrum of the phase quadrature $p_{out}(t)$ of the outgoing light field, as monitored by homodyne detection.

detectability in conventional matter-wave interferometry [9,19], where the particle is smaller than the delocalization of its motional quantum state. Moreover, our results illustrate that, for truly macroscopic bodies, the CSL scaling is carefully balanced: it rapidly restores classicality, while going practically unnoticed in the presence of a thermal environment.

It is clear from Eq. (5) that a narrow linewidth (i.e., a low frequency Ω and a high quality factor $Q = \Omega/\gamma$) is crucial for observing CSL noise against the thermal background. In addition, one must maintain a low temperature of the environment and monitor it precisely and independently of the noise level. Figure 2 illustrates which masses m and linewidths γ are required to test given values of the localization rate λ_{CSL}. We choose a cubic silicon oscillator (side length b, mass density $\varrho = 2300$ kg/m^3) at the temperature $T = 1$ K. With a $\Omega = 1$ Hz, $Q = 10^6$, 1 μg oscillator, one could test λ_{CSL} values as small as 1 nHz, which matches currently estimated bounds. The best sensitivity is obtained with oscillators of roughly the same size as r_{CSL}. Since the approximation (2) for the geometry factor α_{cube} fails in this case, we used the exact expression given in Ref. [44].

Effect of measurement noise.—Thermal noise is not the only limitation for detecting collapse-induced diffusion. The measurement process itself contributes backaction and shot noise to the readout signal [23–26]. In optomechanics the mechanical resonator acts as a refractive (or reflective) element for optical fields. Its quadratures can thus be monitored by coupling the mechanical mode to a driven high-finesse cavity light mode. The momentum diffusion of the oscillator can then be inferred from a continuous interferometric measurement of its position [23]. In the simplest scenario, as sketched in Fig. 1, the phase
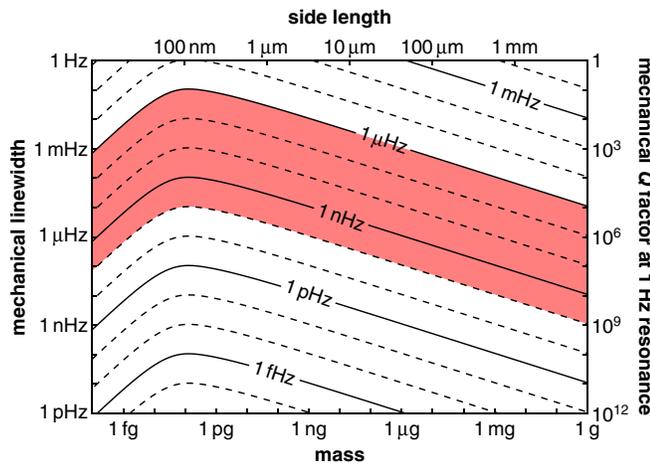

FIG. 2 (color online).   Lower bound Λ_T for the detectable CSL rate parameter λ_{CSL} due to thermal noise at 1 K, for varying mass m and linewidth γ of a cubic silicon cantilever; see Eq. (5). The side length of the cube is given on the top, the quality factor Q of a 1 Hz oscillator on the right. The currently estimated upper bound for λ_{CSL} (0.1 nHz − 1 μHz) is indicated by the shaded area.

quadrature of a light field (relative to its coherent steady-state amplitude) will receive a signal linear in the oscillator's position, $p_{out}(t) = p_{in}(t) + gx(t)$. Here $p_{in}(t)$ is white measurement shot noise, $\langle p_{in}(t)p_{in}(t')\rangle = \frac{1}{2}\delta(t - t')$. The strength of position transduction (of dimension Hz$^{1/2}$ m^{-1}) is given by $g = k\sqrt{\mathcal{F}\Phi}$ in a typical optomechanical setup, where k is the wave number of light, $\mathcal{F}$ is the finesse of the cavity, and $\Phi = P/\hbar\omega_{opt}$ is the photon flux for a power P injected into the interferometer [23].

The mechanical oscillator will in turn be affected by a measurement backaction force proportional to the amplitude quadrature fluctuations $x_{in}(t)$ of the light (again white noise), so that the momentum Langevin equation (4) becomes

$$\dot{p} = -m\Omega^2 x - \gamma p + f_T(t) + f_{CSL}(t) + \hbar g x_{in}(t). \quad (6)$$

The Fourier components of the phase quadrature measured in the outgoing light field are then

$$p_{out}(\omega) = p_{in}(\omega) + g\chi(\omega)[f_T(\omega) + f_\lambda(\omega) + \hbar g x_{in}(\omega)], \quad (7)$$

where the mechanical susceptibility at measurement frequency ω takes the known Lorentzian form $m\chi(\omega) = (\Omega^2 - \omega^2 + i\omega\gamma)^{-1}$. From the measured phase quadrature we can infer the total diffusion force at its Fourier frequency ω,

$$f(\omega) = \frac{p_{out}(\omega)}{g\chi(\omega)}$$

$$= f_{CSL}(\omega) + f_T(\omega) + \frac{p_{in}(\omega)}{g\chi(\omega)} + \hbar g x_{in}(\omega). \quad (8)$$

In this expression, the CSL-induced diffusion force competes with three unavoidable contributions to the signal fluctuation: thermal noise, shot noise, and measurement backaction noise. The corresponding noise spectral density, as obtained from the recorded spectrum of the measurement signal, is

$$S_f(\omega) = D_{CSL} + 2\gamma m k_B T + \frac{1}{2g^2|\chi(\omega)|^2} + \frac{\hbar^2 g^2}{2}$$

$$\geq D_{CSL} + 2\gamma m k_B T + \hbar|\chi(\omega)|^{-1}. \quad (9)$$

Here, the bound is achieved through optimization with respect to g (i.e., laser power P); it represents the standard quantum limit (SQL) of the continuous force measurement [23–26], achieved for $g_{SQL} = 1/\sqrt{\hbar|\chi(\omega)|}$.

As discussed above, it will be advantageous to work with a low-frequency (Hz or sub-Hz), high-Q oscillator to minimize the thermal noise contribution. For suitable measurement frequencies in the kHz range, we can therefore assume $\omega \gg \Omega, \gamma$, so that the high-frequency (free-mass) limit of the susceptibility applies, $|\chi(\omega)| \simeq 1/m\omega^2$.
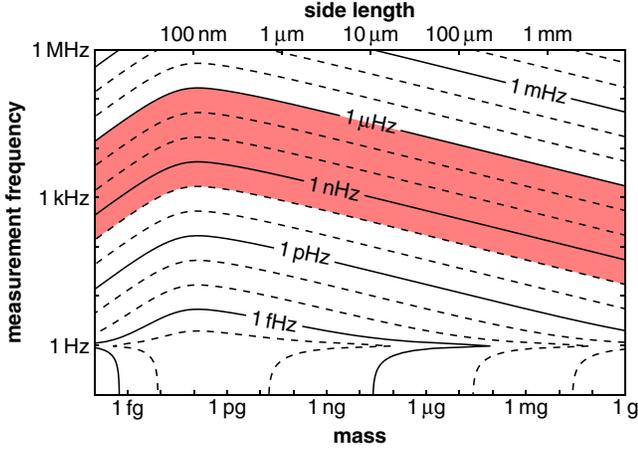
FIG. 3 (color online). Lower bound Λ_{SQL} for the detectable CSL rates λ_{CSL} due to measurement noise at SQL, as a function of mass m and measurement frequency ω; see Eq. (10). We assume a cubic silicon cantilever (side length on the top) with frequency $\Omega = 1$ Hz and quality factor $Q = 10^6$. Relevant upper bounds for the CSL rate are indicated by the shaded area.

Note that this corresponds to the standard limit considered in gravitational wave detection [25,26]. In order to have the CSL diffusion dominate over the measurement-induced diffusion, the first term in Eq. (9) must be larger than the last SQL term,

$$\Lambda_{SQL} \equiv \frac{r_{CSL}^2 \omega^2}{\hbar} \frac{m}{\alpha} < \lambda_{CSL}, \tag{10}$$

for the considered measurement frequency ω. As in the case of the thermal bound (5), this lower bound for detectable CSL rate parameters increases with mass due to the sublinear mass scaling of the geometry parameter α.

Figure 3 illustrates when CSL diffusion will be detectable on top of measurement noise, at given measurement frequencies ω and masses m of a cubic cantilever. For a μg oscillator, sensitivities down to $\lambda_{CSL} > \Lambda_{SQL} \simeq 1$ nHz can be maintained at measurement frequencies up to hundreds of Hz. The SQL coupling frequency in the free-mass limit, $g_{SQL} = \omega\sqrt{m/\hbar}$, is equivalent to a laser power $P_{SQL} = mc^2\omega^2/\mathcal{F}\omega_{opt}$. Several recent experiments

demonstrated backaction noise-limited detection with optomechanical systems [27–29], including a mg-scale mirror [30]. The SQL will eventually be reached by further reducing thermal background noise, and possibly be overcome using Heisenberg-limited measurement strategies [25].

In summary, both the thermal bound (5) and the measurement bound (10) must be taken into account when probing CSL diffusion in optomechanical systems. The sum of both sets the achievable sensitivity in a given setup at SQL. In Table I we list the sensitivities reachable in a number of existing, proposed, and hypothetical configurations. We find that the current experimental state of the art is yet incapable of testing the CSL model at the relevant parameter range of $\lambda_{CSL} < 10^{-8\pm2}$ Hz. To reach the desired sensitivity, one must aim for substantially improved quality factors and temperature control, rather than for high masses.

Bounds for the DP gravitational collapse model.— Compared to CSL, the Diósi-Penrose model exhibits a different mass dependence of the collapse effect, which is related to the gravitational self-energy of the mass distribution $\varrho(r)$ [14,16]. The DP counterpart of the CSL diffusion rate reads as

$$D_{DP} = \frac{G\hbar}{2\pi^2} \int d^3k \frac{k_x^2}{\boldsymbol{k}^2} |\tilde{\varrho}(\boldsymbol{k})|^2, \tag{11}$$

with G the gravitational constant. Although this equation involves only natural constants, one must introduce a blurring parameter $\sigma_{DP} > 0$ to account for the fact that the DP collapse effect diverges for point masses [9,46]. This implies that the DP effect depends not only on the macroscopic geometry of a given piece of matter, but is also highly sensitive to its microscopic lattice structure. That is, a cantilever can be assumed neither a homogeneous nor a rigid body.

We model each nucleus in the crystal lattice as a Gaussian mass distribution of width σ_{DP}, which determines the value of the DP diffusion rate (11) and can therefore be probed with optomechanical systems. For simplicity, we focus on monoatomic cubic lattices with lattice constant $a \gg \sigma_{DP}$, where the DP diffusion rate reduces to the mass-proportional expression [44]

TABLE I. CSL sensitivities for a selection of optomechanical setups with density ϱ, mass m, mechanical frequency Ω, quality factor Q, and temperature T. The thermal sensitivity Λ_T and the measurement-induced sensitivity Λ_{SQL} (at measurement frequency ω) are given in Eqs. (5) and (10), respectively. For simplicity, all systems are assumed to be center-of-mass oscillators, ignoring the specific mode profiles in Refs. [29,30,43]; the hypothetical setup is extrapolated from Ref. [30], using a disk radius of 0.4 mm and thickness of 0.1 mm. A significant test of CSL requires $\Lambda_{T,SQL} < 10^{-8\pm2}$ Hz.

System	ϱ (g/cm³)	m	$\Omega/2\pi$ (Hz)	Q	T (K)	$\omega/2\pi$ (Hz)	Λ_T (Hz)	Λ_{SQL} (Hz)
Gravitational wave detector [33]	2.3	40 kg	1	25000	300	1000	2×10^{-1}	3×10^{-4}
Suspended disk [30]	2.0	5 mg	0.5	5×10^5	300	500	5×10^{-6}	1×10^{-7}
Hypothetical setup	2.0	100 μg	0.1	10^6	0.2	100	2×10^{-10}	2×10^{-9}
SiN membrane [29]	3.4	34 ng	1.6×10^6	1100	4.9	1.6×10^6	4×10^{-1}	3×10^{-6}
Aluminum membrane [43]	2.7	48 pg	1.1×10^7	3.3×10^5	0.015	1.1×10^7	1×10^{-5}	2×10^{-7}

$$D_{DP} \approx \frac{G\hbar}{6\sqrt{\pi}} \left(\frac{a}{\sigma_{DP}}\right)^3 \varrho m. \qquad (12)$$

The greatest detectable blurring parameter Σ_{DP} in the presence of thermal and measurement-induced noise is then mass *independent*,

$$\sigma_{DP} < \Sigma_{DP} \equiv \left[\frac{G\hbar\varrho}{6\sqrt{\pi}(\hbar\omega^2 + 2\gamma k_B T)}\right]^{1/3} a. \qquad (13)$$

Hence, also in this case one does not gain sensitivity by increasing the oscillator's mass.

Conclusion.—We identified the generic sensitivity requirements for detecting stochastic collapse models in optomechanical setups. Since the predicted diffusion competes with inevitable thermal and measurement-induced noise, a high degree of experimental precision and control is crucial. A heavy oscillator, on the other hand, does not improve the sensitivity, even though the collapse-induced diffusion amplifies with mass: The contributions of thermal, backaction and shot noise grow in proportion to mass, whereas the growth of collapse-induced noise is generally weaker.

Our results show that one should rather aim for high quality factors, low and independently measured temperatures, and low oscillation frequencies. Precision experiments with micromechanical oscillators are insofar complementary to interferometric tests with delocalized nanoparticles [18–21], where mass always matters.

[1] K. Hammerer, A. S. Sörensen, and E. S. Polzik, Rev. Mod. Phys. **82**, 1041 (2010).
[2] F. De Martini and F. Sciarrino, Rev. Mod. Phys. **84**, 1765 (2012).
[3] J.-W. Pan, Z.-B. Chen, C.-Y. Lu, H. Weinfurter, A. Zeilinger, and M. Zukowski, Rev. Mod. Phys. **84**, 777 (2012).
[4] M. Arndt and K. Hornberger, Nat. Phys. **10**, 271 (2014).
[5] E. Joos, H. D. Zeh, C. Kiefer, D. Giulini, J. Kupsch, and I.-O. Stamatescu, *Decoherence and the Appearance of a Classical World in Quantum Theory* (Springer, Berlin, 2003).
[6] W. Zurek, Rev. Mod. Phys. **75**, 715 (2003).
[7] M. Schlosshauer, Rev. Mod. Phys. **76**, 1267 (2005).
[8] A. J. Leggett, J. Phys. Condens. Matter **14**, R415 (2002).
[9] A. Bassi and G. Ghirardi, Phys. Rep. **379**, 257 (2003).
[10] G. C. Ghirardi, P. Pearle, and A. Rimini, Phys. Rev. A **42**, 78 (1990).
[11] A. Bassi, K. Lochan, S. Satin, T. P. Singh, and H. Ulbricht, Rev. Mod. Phys. **85**, 471 (2013).
[12] S. L. Adler, *Quantum Theory as an Emergent Phenomenon: The Statistical Mechanics of Matrix Models as the Precursor of Quantum Field Theory* (Cambridge University Press, Cambridge, England, 2004).
[13] S. Nimmrichter and K. Hornberger, Phys. Rev. Lett. **110**, 160403 (2013).
[14] L. Diósi, Phys. Lett. A **120**, 377 (1987).
[15] L. Diósi, Phys. Rev. A **40**, 1165 (1989).
[16] R. Penrose, Gen. Relativ. Gravit. **28**, 581 (1996).
[17] W. Marshall, C. Simon, R. Penrose, and D. Bouwmeester, Phys. Rev. Lett. **91**, 130401 (2003).
[18] O. Romero-Isart, A. C. Pflanzer, F. Blaser, R. Kaltenbaek, N. Kiesel, M. Aspelmeyer, and J. I. Cirac, Phys. Rev. Lett. **107**, 020405 (2011).
[19] S. Nimmrichter, K. Hornberger, P. Haslinger, and M. Arndt, Phys. Rev. A **83**, 043621 (2011).
[20] K. Hornberger, S. Gerlich, P. Haslinger, S. Nimmrichter, and M. Arndt, Rev. Mod. Phys. **84**, 157 (2012).
[21] J. Bateman, S. Nimmrichter, K. Hornberger, and H. Ulbricht, arXiv:1312.0500.
[22] M. Bahrami, M. Paternostro, A. Bassi, and H. Ulbricht, Phys. Rev. Lett. **112**, 210404 (2014).
[23] A. A. Clerk, M. H. Devoret, S. M. Girvin, F. Marquardt, and R. J. Schoelkopf, Rev. Mod. Phys. **82**, 1155 (2010).
[24] M. Aspelmeyer, T. J. Kippenberg, and F. Marquardt, arXiv:1303.0733 [Rev. Mod. Phys. (to be published)].
[25] S. L. Danilishin and F. Y. Khalili, Living Rev. Relativity **15** (2012).
[26] Y. Chen, J. Phys. B **46**, 104001 (2013).
[27] K. W. Murch, K. L. Moore, S. Gupta, and D. M. Stamper-Kurn, Nat. Phys. **4**, 561 (2008).
[28] A. H. Safavi-Naeini, J. Chan, J. T. Hill, Thiago P. Mayer Alegre, A. Krause, and O. Painter, Phys. Rev. Lett. **108**, 033602 (2012).
[29] T. P. Purdy, R. W. Peterson, and C. A. Regal, Science **339**, 801 (2013).
[30] N. Matsumoto, Y. Michimura, G. Hayase, Y. Aso, and K. Tsubono, arXiv:1312.5031.
[31] C. Caves, K. Thorne, R. Drever, V. Sandberg, and M. Zimmermann, Rev. Mod. Phys. **52**, 341 (1980).
[32] C. M. Caves, Phys. Rev. D **23**, 1693 (1981).
[33] H. Müller-Ebhardt, H. Rehbein, R. Schnabel, K. Danzmann, and Y. Chen, Phys. Rev. Lett. **100**, 013601 (2008).
[34] H. Miao, S. Danilishin, H. Müller-Ebhardt, H. Rehbein, K. Somiya, and Y. Chen, Phys. Rev. A **81**, 012114 (2010).
[35] A. Bassi, E. Ippoliti, and S. Adler, Phys. Rev. Lett. **94**, 030401 (2005).
[36] Q. Fu, Phys. Rev. A **56**, 1806 (1997).
[37] S. L. Adler and F. M. Ramazanolu, J. Phys. A **40**, 13395 (2007).
[38] W. Feldmann and R. Tumulka, J. Phys. A **45**, 065304 (2012).
[39] S. L. Adler, J. Phys. A **40**, 2935 (2007).
[40] D. E. Chang, C. A. Regal, S. B. Papp, D. J. Wilson, J. Ye, O. Painter, H. J. Kimble, and P. Zoller, Proc. Natl. Acad. Sci. U.S.A. **107**, 1005 (2010).
[41] O. Romero-Isart, M. L. Juan, R. Quidant, and J. I. Cirac, New J. Phys. **12**, 033015 (2010).
[42] J. D. Thompson, B. M. Zwickl, A. M. Jayich, F. Marquardt, S. M. Girvin, and J. G. E. Harris, Nature (London) **452**, 72 (2008).
[43] J. D. Teufel, T. Donner, D. Li, J. W. Harlow, M. S. Allman, K. Cicak, A. J. Sirois, J. D. Whittaker, K. W. Lehnert, and R. W. Simmonds, Nature (London) **475**, 359 (2011).
[44] See Supplemental Material at http://link.aps.org/supplemental/10.1103/PhysRevLett.113.020405 for details on the collapse-induced diffusion rates.
[45] Although we focus on center-of-mass oscillations, the considered collapse models should imply a similar size dependence for other mechanical modes with smaller effective masses.
[46] G. C. Ghirardi, R. Grassi, and A. Rimini, Phys. Rev. A **42**, 1057 (1990).